TRANSACTIONS OF THE
AMERICAN MATHEMATICAL SOCIETY
Volume 289, Number 1, May 1985

A NONSHRINKABLE DECOMPOSITION OF S^3 WHOSE NONDEGENERATE ELEMENTS ARE CONTAINED IN A CELLULAR ARC

BY

W. H. ROW AND JOHN J. WALSH[1]

ABSTRACT. A decomposition G of S^3 is constructed with the following properties:

(1) The set N_G of all nondegenerate elements consists of a null sequence of arcs and $J = \mathrm{CL}(\cup\{g \in N_G\})$ is a simple closed curve.

(2) Each arc contained in J is cellular.

(3) J is the boundary of a disk Q that is locally flat except at points of J.

(4) The decomposition G is not shrinkable; that is, the decomposition space is not homeomorphic to S^3.

1. Introduction. This paper presents a decomposition G of S^3 into points and a null sequence of cellular arcs that is not shrinkable, i.e., the decomposition space S^3/G is not homeomorphic to S^3. The decomposition has several noteworthy features: the nondegenerate elements of G are contained in a simple closed curve J, each arc contained in J is cellular, and J is the boundary of a disk that is locally flat except at points of J.

The earliest example of a nonshrinkable decomposition of S^3 that consists of points and a null sequence of cellular sets is due to R. H. Bing [**Bi**]. An improvement was announced in 1963 by D. S. Gillman and J. M. Martin [**GM**], where their nondegenerate elements were cellular arcs. In 1977 R. H. Bing and M. Starbird [**BS**] produced and published the details of such an example. The latter example, with minor modifications in its construction, has its nondegenerate elements contained in an arc, but the individual decomposition elements and their subarcs are essentially the only cellular subarcs. One cannot insist there be less "subcellularity" as subarcs of cellular arcs are cellular (see [**Mc**] for $n \neq 4$ and [**Fr**] for $n = 4$).

In higher dimensions, the existence of nonshrinkable decompositions of S^n consisting of points and a null sequence of cellular sets was established by R. J. Daverman [$\mathbf{Da_1}$] for $n \geq 5$ and D. G. Wright [**Wr**] for $n = 4$. Specific examples of nonshrinkable decompositions of S^n ($n \geq 3$) in which the nondegenerate elements form a null sequence of cellular arcs were exhibited by the second author and R. J. Daverman [**DW**]. The examples have the feature that the nondegenerate elements are contained in a 1-dimensional compact subset of a (noncellular) 2-cell. In general, it is not possible to replace the 2-cell with an arc. Pointed out in [**DW**, §5] is that for

Received by the editors April 27, 1983 and, in revised form, May 22, 1984.

1980 *Mathematics Subject Classification*. Primary 57A10, 57A60; Secondary 54B10, 55A30.

Key words and phrases. Cellular decomposition, cellular arc, nonshrinkable, 3-manifold.

[1]Research partially supported by a National Science Foundation Grant; Alfred P. Sloan Fellow

0002-9947/85 $1.00 + $.25 per page

$n \geq 5$ the decomposition of S^n having nondegenerate elements contained in a finite graph satisfies the Disjoint Disks Property. The latter is a property which R. D. Edwards showed implies the shrinkability of cell-like decompositions [**Ed**].

MAIN THEOREM. *There is a decomposition G of S^3 that satisfies*:

(1) *the nondegenerate elements $N_G = \{ g \in G: g \neq \text{point} \}$ form a null sequence of arcs and $J = \mathrm{CL}(\cup\{ g \in N_G \})$ is a simple closed curve*;

(2) *each arc contained in J is cellular*;

(3) *J is the boundary of a disk Q that is locally flat except at points of J*;

(4) *the decomposition space S^3/G is not homeomorphic to S^3.*

The example described in the title answers a question that has circulated for several years (e.g., [$\mathbf{Da_2}$]) and, to our knowledge, was first raised by C. D. Bass. Specifically, a decomposition $\tilde{G}$, determined by choosing any $g_0 \in N_G$ and insisting that $N_{\tilde{G}} = N_G - \{ g_0 \}$, is not shrinkable and $\mathrm{CL}(\cup\{ g \in N_{\tilde{G}} \})$ is a cellular arc.

COROLLARY 1. *There is a nonshrinkable decomposition of S^3 whose nondegenerate elements are contained in a cellular arc.*

There are other examples that can be exhibited by manipulating the decomposition G; some of these are listed below and discussed in §5. We thank R. J. Daverman for bringing these to our attention.

COROLLARY 2. *There is a nonshrinkable decomposition of S^3 whose nondegenerate elements form a null sequence of cellular disks (resp., 3-cells) that are contained in a cellular disk (resp., 3-cell).*

COROLLARY 3. *There is a nonshrinkable decomposition of S^3 whose nondegenerate elements are contained in a cellular arc A that lies in the boundary of a cellular disk.*

COROLLARY 4. *There is an embedding e: $I^2 \to S^3$ ($I = [0,1]$) such that $e(I^2)$ is cellular but the decomposition H determined by requiring that $N_H = \{ e(I \times \{t\}): 0 \leq t \leq 1 \}$ is not shrinkable.*

We acknowledge the contribution of S. Pax who participated in several discussions during the Summer of 1981 that set forth the rudimentary strategy for building the example.

2. Description of the example. An *ε-chambered circular chain*, as illustrated in Figure 1, consists of:

(i) *chambers*: a finite collection of 3-cells and solid tori, each having diameter less than ε, that can be ordered, say $c_0, c_1, \ldots, c_n$, so that $c_0 \cap c_n = \partial c_0 \cap \partial c_n$ is a disk, $c_j \cap c_{j+1} = \partial c_j \cap \partial c_{j+1}$ is a disk for $0 \leq j \leq n-1$, and $c_k \cap c_j = \varnothing$ $(k \neq j)$ otherwise;

(ii) *edges*: a finite collection, say $e_1, \ldots, e_L$, of pairwise disjoint sets each of which is the union of at least five consecutive chambers with the first and last chamber being a 3-cell and with a 3-cell chamber lying between any two solid tori chambers;

(iii) *vertices*: a finite collection, say $v_1,\ldots,v_L$, of pairwise disjoint 3-cell chambers such that $v_1 \cap e_1 = \partial v_1 \cap \partial e_1$ and $v_1 \cap e_L = \partial v_1 \cap \partial e_L$ are disks and $v_j \cap e_{j-1} = \partial v_j \cap \partial e_{j-1}$ and $v_j \cap e_j = \partial v_j \cap \partial e_j$ are disks for $2 \leqslant j \leqslant L$.

Evidently, each chamber is either a vertex or is contained in an edge.

We begin the construction of the decomposition G by specifying a solid torus $\mathscr{C}(0)$ standardly embedded in S^3, a simple closed curve $J_0 \subset \partial\mathscr{C}(0)$ that is homotopically essential in $\mathscr{C}(0)$ and that bounds a PL disk Q_0 with $Q_0 \cap \mathscr{C}(0) = J_0$, and a slightly enlarged copy K of $\mathscr{C}(0)$. For $k \geqslant 1$, we shall specify a sequence of positive numbers $\varepsilon_1, \varepsilon_2, \ldots$ converging to zero and a sequence of sets $\mathscr{C}(k)$ having the following properties:

(1) $\mathscr{C}(k) \subset \mathscr{C}(k-1)$ and $\mathscr{C}(k)$ is an ε_k-chambered circular chain having 2^k edges and 2^k vertices.

(2) The collection of edges of $\mathscr{C}(k)$ has the Two Disks Property with respect to K (the Two Disks Property will be defined later).

(3) Each edge of $\mathscr{C}(k)$ is standardly embedded in $\mathscr{C}(k-1)$ (precisely what is meant by the latter will be made clear during the course of the construction).

(4) Each chamber of $\mathscr{C}(k)$ is contained in a chamber of $\mathscr{C}(k-1)$.

(5) There is a simple closed curve $J_k \subset \partial\mathscr{C}(k)$, meeting each chamber of $\mathscr{C}(k)$ in an arc, that bounds a PL disk $Q_k \subset \mathrm{CL}(S^3 - \partial\mathscr{C}(k))$ that is obtained from Q_{k-1} by attaching $3\varepsilon_{k-1}$-small disjoint PL disks along subarcs of J_{k-1}.

(6) $\mathscr{C}(k)$ goes "straight through" the chambers of $\mathscr{C}(k-1)$; more precisely, if r: $J_k \to J_{k-1}$ is the restriction of a chamber invariant retraction of $\mathscr{C}(k-1)$ onto J_{k-1}, then, for any two consecutive chambers C_0 and C_1 of $\mathscr{C}(k-1)$, there is exactly one component of $r^{-1}(J_{k-1} \cap (C_0 \cup C_1))$ that r maps onto the subarc $J_{k-1} \cap (C_0 \cup C_1)$.

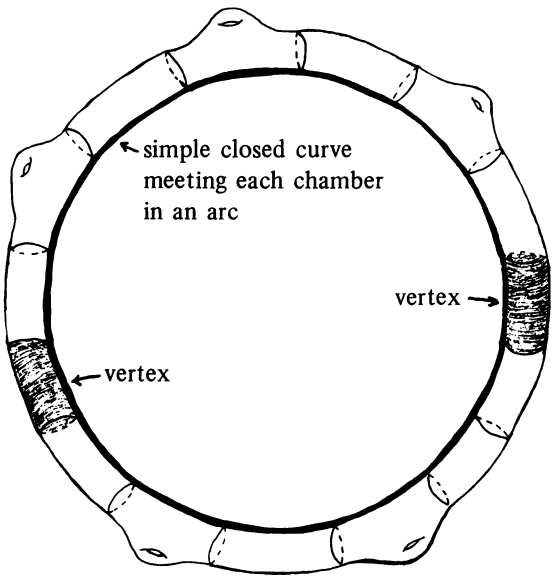

FIGURE 1. ϵ-chambered circular chain with two edges and two vertices.

(7) Each edge e of $\mathscr{C}(k-1)$ gives rise to a single edge e' of $\mathscr{C}(k)$ with $e' \subset$ PL 3-cell $\subset e$.

(8) Each vertex v of $\mathscr{C}(k-1)$ gives rise to a single edge e' of $\mathscr{C}(k)$ with $e' \subset v \cup c \cup \tilde{c}$, where c and $\tilde{c}$ are the chambers of $\mathscr{C}(k-1)$ adjacent to v (consequently, $v \cup c \cup \tilde{c}$ is a PL 3-cell) and, furthermore, the two vertices v', v'' of $\mathscr{C}(k)$ adjacent to e' are contained in v.

(9) For a string $e_0, v_1, e_1, v_2, e_2, \ldots, e_L$ of distinct but consecutive edges and vertices of $\mathscr{C}(k-1)$ (i.e., $v_i \cap e_{i-1} \neq \varnothing$ and $v_i \cap e_i \neq \varnothing$), the corresponding string $e'_0, v'_1, e'_1, v'_2, e'_2, \ldots, v'_{2L}, e'_{2L}$ of edges and vertices of $\mathscr{C}(k)$ determined by conditions (7) and (8) satisfies a containment

$$e'_0 \cup v'_1 \cup e'_1 \cup \cdots \cup v'_{2L} \cup e'_{2L} \subset \text{PL 3-cell} \subset e_0 \cup v_1 \cup \cdots \cup v_L \cup e_L.$$

Except for condition (2), these conditions are immediate consequences of or follow easily from the construction of the $\mathscr{C}(k)$'s described in the next section. Establishing the Two Disks Property is the difficult step, the entirety of §4 being needed to verify that condition (2) is met. The remainder of this section is devoted to giving a description of the example G and an outline of the proofs of the four properties of G claimed in the Main Theorem.

The simple closed curve J is easily determined by setting $J = \bigcap \mathscr{C}(k)$, conditions (1), (4) and (6) ensuring that this intersection is a simple closed curve. The disk that J bounds that is locally flat except at points of J is obtained as $Q = J \cup (\bigcup Q_k)$, where the Q_k's are specified in condition (5) (a conclusive argument that Q is a disk may depend on specifics from the construction of the $\mathscr{C}(k)$'s in the next section).

The nondegenerate elements of G arise as nested intersections of edges of the $\mathscr{C}(k)$'s. Precisely, given an edge e_k of $\mathscr{C}(k)$, condition (7) specifies an edge e_{k+1} of $\mathscr{C}(k+1)$ with $e_{k+1} \subset e_k$ and, recursively, a sequence of edges e_{k+j} of $\mathscr{C}(k+j)$ with $e_k \supset e_{k+1} \supset \cdots \supset e_{k+j} \supset \cdots$. The intersection $\bigcap_{j=0}^{\infty} e_{k+j}$ determines a nondegenerate element of G, the totality of the nondegenerate elements of G being all such intersections. The two edges of $\mathscr{C}(1)$ produce 2 nondegenerate elements of G, the edges of $\mathscr{C}(2)$ give rise to 2 additional nondegenerate elements of G having diameters $< 3\varepsilon_1$, and, in general, the edges of $\mathscr{C}(k)$ give rise to 2^{k-1} additional nondegenerate elements of G having diameters $< 3e_{k-1}$. In particular, G is a null-sequence decomposition.

In the presence of conditions (7) and (8), since the vertices of $\mathscr{C}(k)$ are pairwise disjoint and have diameters $< \varepsilon_k$, it follows that $\mathrm{CL}(\bigcup\{ g \in N_G \}) = J$. The containment "$e' \subset$ PG 3-cell $\subset e$" stated in condition (7) immediately establishes that each nondegenerate element of G is cellular.

Based on the property of the $\mathscr{C}(k)$'s set forth in condition (9), we are able to show the following constrained version of the second property stated in the Main Theorem.

(2)′ *Each subarc of J that misses at least one nondegenerate element of G is cellular.*

The relatively easy verification that each subarc of J is cellular appears at the end of the next section and involves details of the construction in addition to those

abstracted above. Returning to the verification of (2)′: First note that any consecutive string of edges and vertices of a $\mathscr{C}(k-1)$ as in condition (9) recursively gives rise to a nested intersection of the union of such strings, one from each $\mathscr{C}(k-1+j)$ for $j = 0, 1, 2, \ldots$; the 3-cells specified in condition (9) establish the cellularity of the subarc of J that is this intersection. Second, any subarc of J missing a nondegenerate element is contained in a subarc of J of the type just described. Third, recall that any subarc of a cellular arc is cellular [**Mc**].

Before ending this section with a discussion of the Two Disks Property and of the fact that S^3/G is not homeomorphic to S^3 (or, equivalently, that G is not a shrinkable decomposition [**Ar**]), we point out that property (2)′ is sufficient to insure the existence of a nonshrinkable decomposition of S^3 all of whose nondegenerate elements lie in a cellular arc as in Corollary 1. Write $J = A_1 \cup A_2$ as the union of two subarcs, where $A_1 \cap A_2$ consists of two points, both being degenerate elements of G. Then both arcs A_1 and A_2 are cellular and one of the decompositions G_1 (resp., G_2) whose nondegenerate elements consist precisely of the nondegenerate elements of G contained in A_1 (resp., A_2) is not shrinkable. For otherwise, carefully chosen shrinking homeomorphisms for G_1 and G_2 could be combined to produce a shrinking homeomorphism for G.

The final goal of this section is to observe that condition (2) ensures that S^3/G is not homeomorphic to S^3. Recall that, for the solid torus K, there is exactly one PL disk $E \subset K$ up to PL-isotopy such that $E \cap \partial K = \partial E$ is a homotopically essential curve in ∂K; such a disk is called a *meridional disk* of K. A collection of sets $\{X_i\}$ is said to have the *Two Disks Property* with respect to K provided, given any two disjoint meridional disks E and D of K, there is some X_i that meets both E and D.

If G were a shrinkable decomposition, then there would be two meridional disks E and D such that no element of G meets both E and D (choose disjoint meridional disks E' and D' and set $E = h^{-1}(E')$ and $D = h^{-1}(D')$ for an appropriately chosen shrinking homeomorphism h). There is an integer k such that $3\varepsilon_{k+j} <$ distance between E and D for all $j \geqslant 0$. The only elements of G having diameters larger than $3\varepsilon_k$ are among the 2^k elements of G determined by the edges of $\mathscr{C}(k)$. Since these elements do not meet both E and D, then, for some $j \geqslant 0$, the 2^k edges of $\mathscr{C}(k+j)$ that also determine these elements do not meet both E and D. But this contradicts condition (2) since the remaining edges of $\mathscr{C}(k+j)$ are too small to meet both E and D.

3. Construction of the $\mathscr{C}(k)$'s. A standardly embedded solid torus $\mathscr{C}(0)$, a simple closed curve $J_0 \subset \partial\mathscr{C}(0)$, and a PL disk Q_0 were specified in the preceding section. Figure 2 illustrates the first step in describing $\mathscr{C}(1)$. The two vertices of $\mathscr{C}(1)$ are accurately drawn, each being a relative regular neighborhood with respect to $\mathscr{C}(0)$ of a subarc of J_0 while the pair of subarcs of J_0 remaining, each with an eyeglass attached, serve adequately as cores for the edges of $\mathscr{C}(1)$ for most of our purposes, an adjustment being necessary in order to produce an ε_1-chambering, the simple closed curve J_1, and the small disks that attach to Q_0 to form Q_1. Figure 3 depicts, in order, the core just described, the actual core of an edge of $\mathscr{C}(1)$, the intersection of

J_1 and an edge of $\mathscr{C}(1)$ together with an ε_1-chambering of the edge, and the small disk that is used to enlarge Q_0 and produce Q_1. An important point is that the two edges of $\mathscr{C}(1)$ have the Two Disks Property with respect to K (the slightly enlarged copy of $\mathscr{C}(0)$ specified in the preceding section), provided the two cores portrayed in Figure 2 have the property. An analysis of the double cover of K appearing in [**BS**] establishes the property for these cores.

Before proceeding with the construction of a general $\mathscr{C}(k)$ we make several comments.

COMMENT 1. We shall be content with describing cores of edges as we have done in Figure 2, leaving the reader to make the adjustments described above in order to produce the J_k's, Q_k's and chamberings. In addition to attaching eyeglasses to the J_k's as above, we shall need to attach eyeglasses with an extra dangle. This together with the necessary comparable modifications is portrayed in Figure 4.

COMMENT (2). A $\mathscr{C}(k)$ arises as a relative regular neighborhood of a 1-complex in $\mathscr{C}(k-1)$ that contains part of $J_{k-1} \subset \partial\mathscr{C}(k-1)$ and, consequently, we have only $\mathscr{C}(k) \subset \mathscr{C}(k-1)$ and not $\mathscr{C}(k) \subset \operatorname{Int}\mathscr{C}(k-1)$; this causes no difficulties but is a slight deviation from similar constructions (e.g., [**BS**]).

COMMENT (3). Except for the Two Disks Property stated in condition (2) whose verification fills the next section and condition (9) that is briefly discussed at the end of this section, we leave for the reader to observe that the conditions stated in the last section are, in fact, satisfied.

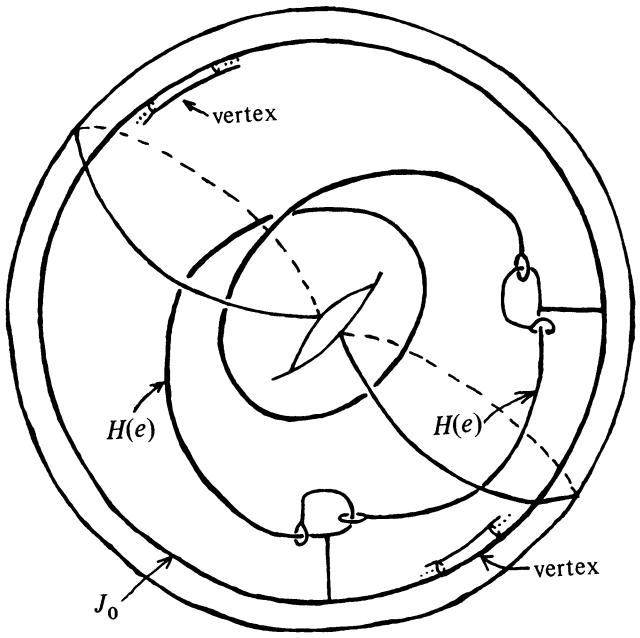

$\mathscr{C}(0)$

FIGURE 2

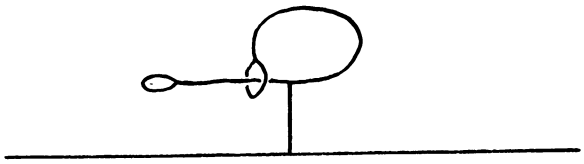

(a) $H(e)$

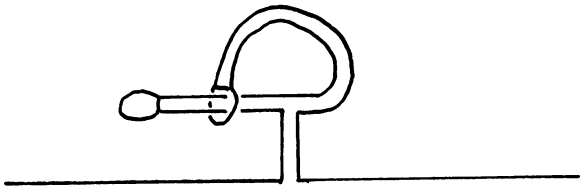

(b) altered $H(e)$

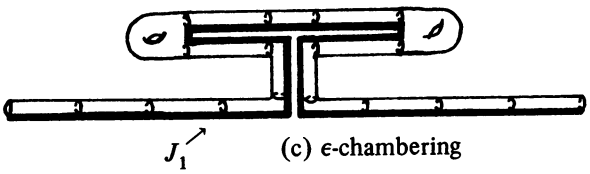

(c) ϵ-chambering

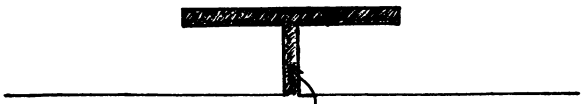

(d) disk attached to Q_0

FIGURE 3

COMMENT (4). The construction that follows uses a large number of eyeglasses with an extra dangle attached to certain eyeglasses as displayed in Figure 5. Notice in Figure 5 that there are "standard" disks associated with each eyeglass; these will always be denoted by the letter B, and there is a "standard" disk associated with each dangle; these will always be denoted by the letter T.

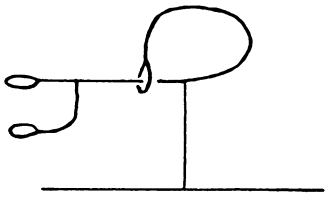

(a) $H(e)$

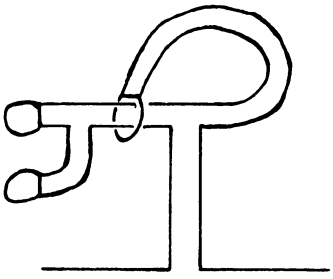

(b) altered $H(e)$

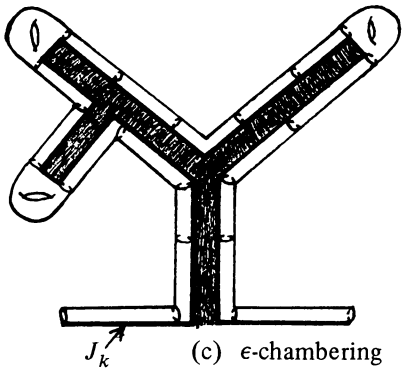

(c) ϵ-chambering

FIGURE 4

COMMENT (5). Observe that for each edge e of $\mathscr{C}(1)$ there is a PL disk $M_e \subset \mathscr{C}(0)$ such that $M_e \cap \partial\mathscr{C}(0) = \partial M_e \cap \partial\mathscr{C}(0)$ is the subarc of J_0 to which an eyeglass is attached to form e and such that M_e contains the eyeglass, the disks added to Q_0 associated with the eyeglass, and a core of e. In fact, we insist that e be a slight "thickening" of $M_e \cap e$. The disk M_e exists since individually each eyeglass "unties" as illustrated in Figure 6; of course, M_e meets the other edge of $\mathscr{C}(1)$. In general, the statement in condition (3) that each edge of $\mathscr{C}(k)$ is "standardly embedded" ensures that there is a comparable PL disk M_e for each edge e of $\mathscr{C}(k)$. The disk M_e shall satisfy the following properties. Depending on whether an edge e' or vertex v of $\mathscr{C}(k-1)$ spawned e, $M_e \subset e'$ or $M_e \subset c \cup v \cup \tilde{c}$, with c, $\tilde{c}$ being the chambers

adjacent to v. Depending again on the same condition, either $M_e \cap \partial e' = \partial M_e \cap \partial e' = J_{k-1} \cap e'$ or $M_e \cap \partial(c \cup v \cup \tilde{c}) = \partial M_e \cap \partial v$, the latter being the subarc of $J_{k-1} \cap v$ to which an eyeglass is attached to form e. The disk M_e contains the disks associated with e that are attached to Q_{k-1} to form Q_k. The intersection $M_e \cap e$ is exactly as illustrated in Figure 7 and e is a slight "thickening" of $M_e \cap e$. The subdisks of M_e that span the "holes" of the solid tori chambers of $\mathscr{C}(k)$ are, in general, quite large; these subdisks contain the intersection of M_e and other edges of $\mathscr{C}(k)$. (In fact, M_e meets only one other edge of $\mathscr{C}(k)$.)

We are ready to start the construction of $\mathscr{C}(k)$, beginning with a description of its edges and vertices.

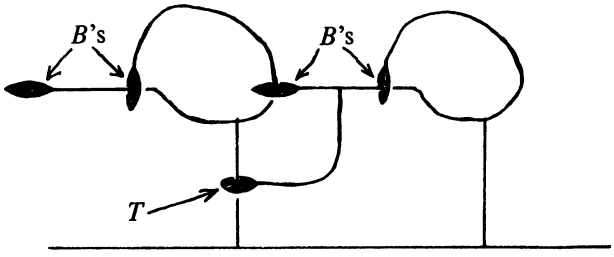

FIGURE 5

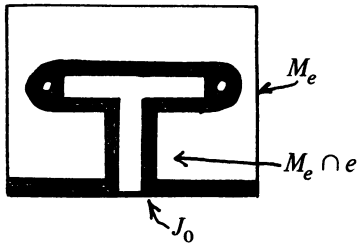

FIGURE 6

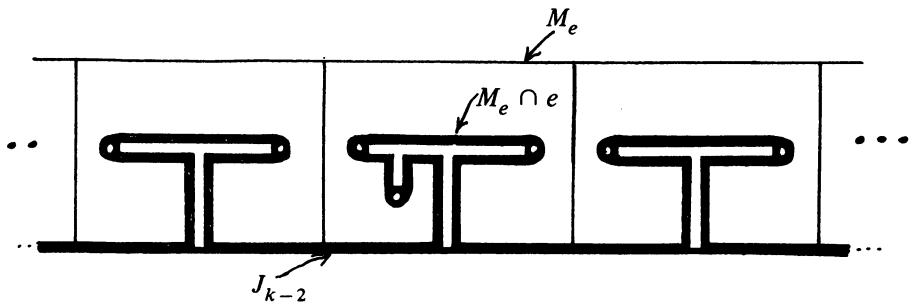

FIGURE 7

Edges of $\mathscr{C}(k)$ *associated with vertices of* $\mathscr{C}(k-1)$. Depicted in Figure 8(a) is a vertex v of $\mathscr{C}(k-1)$ and its two adjacent chambers c, $\tilde{c}$. An eyeglass is attached to a subarc of $J_{k-1} \cap v$ to form the core of an edge of $\mathscr{C}(k)$. The eyeglass is denoted by $G(v)$ and the core by $H(v)$. Portrayed in the chambers c and $\tilde{c}$ is the linking of this edge with edges of $\mathscr{C}(k)$, described next, arising from edges of $\mathscr{C}(k-1)$ adjacent to v. Notice in Figures 8(b) and 8(c) the two vertices of $\mathscr{C}(k)$ associated with v and the ϵ_k-chambering of the edge. The reader should note the existence of a disk as in Comment (5) for the edge. We shall use $\overline{G}(v)$ to denote the eyeglass $G(v)$ together with its associated B's.

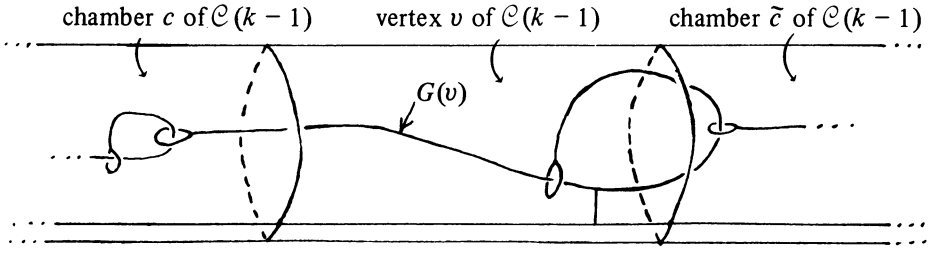

(a)

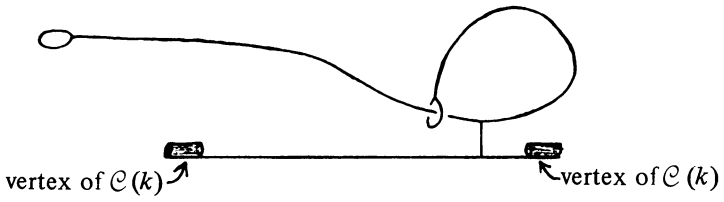

(b) $H(v)$ and adjacent vertices

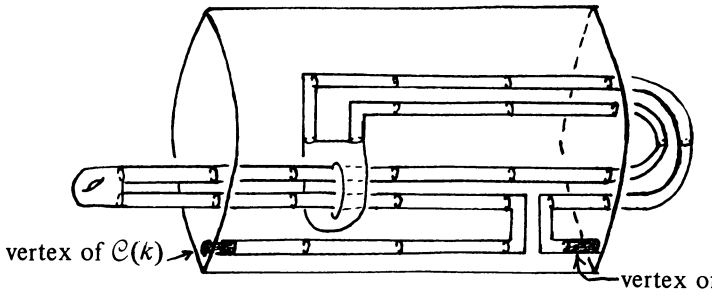

(c) ϵ_k-chambering of altered $H(v)$

FIGURE 8

Edges of $\mathscr{C}(k)$ associated with edges of $\mathscr{C}(k-1)$. Start with an edge e of $\mathscr{C}(k-1)$ and its associated disk M_e. Contained in M_e is a subdisk, named $\tilde{M}_e$, that consists of the disk-with-holes $M_e \cap e$ and the disks "filling these holes". Displayed in Figure 9(a) is $\tilde{M}_e \times I$ and the edge e viewed as $(M_e \cap e) \times I$, together with the chambering of e. (The 3-cell "plugs" attached to e to form $\tilde{M}_e \times I$ are large in size in general.) A "fan" of $2^k + 1$ copies of $\tilde{M}_e$ joined along $J_{k-1} \cap M_e$ together with triangular regions attached at the ends in alternating fashion is depicted in Figure 9(b) along with the "subfan" of copies of $M_e \cap e$. The "fan" is the quotient space obtained by starting with a planar strip of $2^k + 1$ copies of M_e attached along triangular regions as in Figure 10 and making identifications along the base as indicated by the arrows. Proceeding from left to right, the copies of $\tilde{M}_e$ (resp., $M_e \cap e$) are denoted by $\tilde{M}_e(1)$, $\tilde{M}_e(2), \ldots$ (resp., $(M_e \cap e)(1)$, $(M_e \cap e)(2), \ldots$) with each triangular region associated with the copy of $\tilde{M}_e$ (resp., $M_e \cap e$) on its right. The "fan" is inserted into e as

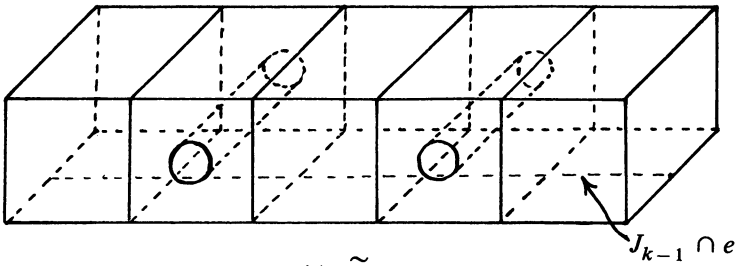

(a) $\tilde{M}_e \times I$

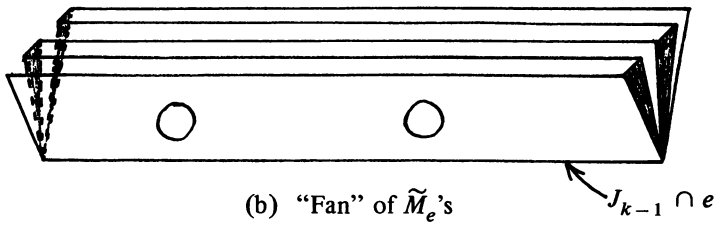

(b) "Fan" of $\tilde{M}_e$'s

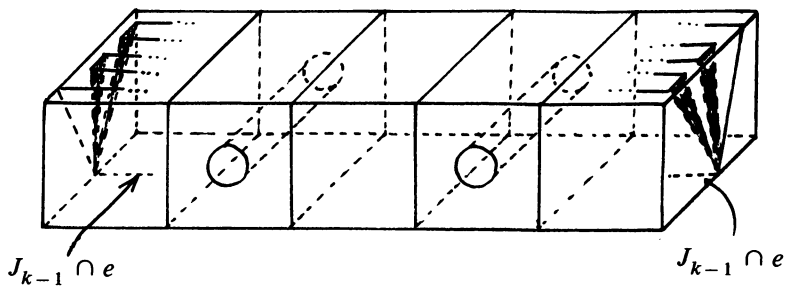

(c) "Fan" inserted in $\tilde{M}_e \times I$

FIGURE 9

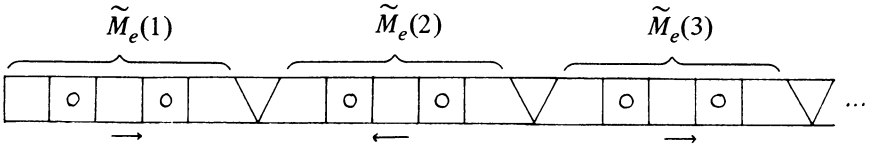

FIGURE 10

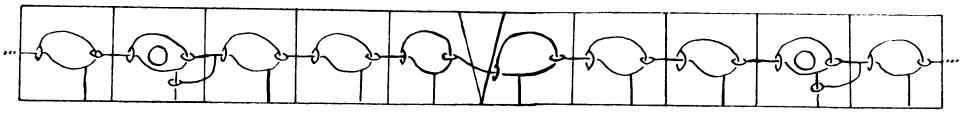

FIGURE 11

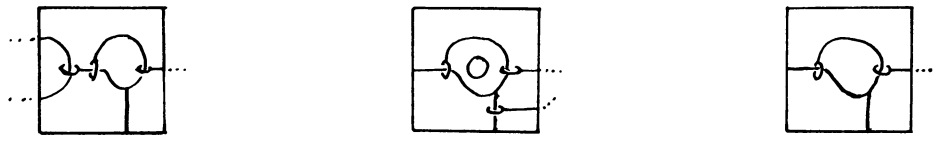

FIGURE 12

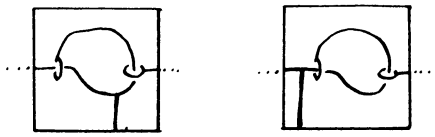

FIGURE 13

indicated in Figure 9(c); notice that the triangular regions have been tilted slightly into e. Before describing the edge of $\mathscr{C}(k)$ spawned by e, the 3-cell chambers of e are subdivided where necessary so that immediately to each side of a torus chamber is a string of at least $k + 2$ 3-cell chambers of e.

A core of the edge of $\mathscr{C}(k)$ spawned by e is described using the planar strip of $2^k + 1$ copies of $M_e \cap e$ attached along triangular regions together with the chambering of it into disks and annuli induced by the chambering of e (each triangular region is combined with the disk to its right so as to form a single chamber). A string of eyeglasses, one for each chamber of the planar strip, is run as depicted in Figure 11; these eyeglasses are contained in a thin neighborhood of the strip. Note that for an annulus chamber the eyeglass, with its associated B's, links the hole of the annulus (Figure 12(b)), that the left-most B associated with the left-most eyeglass meets in a single point the eyeglass that specifies the edge of $\mathscr{C}(k)$ determined by one of the vertices of $\mathscr{C}(k-1)$ adjacent to e (Figure 12(a)), and that the right-most

eyeglass, with its associated B's, links the eyeglass that specifies the edge of $\mathscr{C}(k)$ determined by the other vertex of $\mathscr{C}(k-1)$ adjacent to e (see Figure 12(c)). The string of eyeglasses associated with the chambers of $(M_e \cap e)(i)$ in the planar strip is denoted $G(e,i)$ and these eyeglasses together with their associated B's are denoted $\bar{G}(e,i)$, for $i = 1,\ldots,2^k+1$. A core, denoted by $H(e)$, for the edge of $\mathscr{C}(k)$ spawned by e is obtained by connecting each eyeglass of $\cup\{G(e,i)\colon i = 1,\ldots,2^k+1\}$ to $J_{k-1} \cap e$ with an arc in M_e as depicted in Figure 11 and attaching an extra dangle to each eyeglass associated with a chamber that follows an annulus chamber also as depicted in Figure 11. The core $H(e)$ consists of the eyeglasses constituting the $G(e,i)$'s, the arcs used to attach these to $J_{k-1} \cap e$, the extra dangles, and $J_{k-1} \cap e$. For convenience, we choose the arcs used to attach the eyeglasses to meet $J_{k-1} \cap e$ in distinct points. For important reasons, the arc should meet the eyeglass in the region specified (see Figure 13).

Comments and further notation. In describing the $G(e)$'s and $G(v)$'s we implicity assumed that an orientation on the circular chambering of $\mathscr{C}(k-1)$ was respected so that the eyeglass with its associated B's, namely $\bar{G}(v)$ for v a vertex of $\mathscr{C}(k-1)$, meets in a single point the "final" eyeglass of $G(e)$ as indicated in Figure 12(c) for e the edge of $\mathscr{C}(k-1)$ adjacent to v on v's "left" side and links the "first" eyeglass of $G(e')$ as indicated in Figure 12(a) for e' the edge of $\mathscr{C}(k-1)$ adjacent to v on v's "right" side. In particular, the totality of the eyeglasses, say $G = (\cup_{e,i} G(e,i)) \cup (\cup_v G(v))$, is a circular chain of eyeglasses that winds essentially once around $\mathscr{C}(0)$ (and K). More precisely, G together with the B's associated to the eyeglasses forming G contains a simple closed curve meeting each eyeglass in a subarc and winding once around K. Notice that G completely "unties" if any single eyeglass is removed.

We discussed in the preceding section that the cores of the edges of $\mathscr{C}(k)$, i.e., the $H(e)$'s and $H(v)$'s, must be adjusted as displayed in Figures 3, 4 and 8 so as to produce an ε_k-chambering, the simple closed curve J_k, and the small disks that are attached to Q_{k-1} to produce Q_k. This is probably an appropriate time for the reader to verify that $\mathscr{C}(k)$ satisfies the nine conditions listed in the preceding section except for condition (2) and condition (9) and that the disk M_e for e an edge of $\mathscr{C}(k)$ described earlier in Comment (5) exists.

With regard to condition (2), observe that it suffices to show that the collection $\{H(e)\colon e \text{ an edge of } \mathscr{C}(k-1)\} \cup \{H(v)\colon v \text{ a vertex of } \mathscr{C}(k-1)\}$ has the Two Disks Property with respect to K, a fact that the next section is devoted to establishing.

With regard to condition (9), a property of the $H(e)$'s and $H(v)$'s is described in the final paragraph of this section that establishes not only condition (9) but also the conclusion of the Main Theorem that every subarc of the simple closed curve J is cellular. First, we need additional notation.

The disks denoted by B associated to each eyeglass $G(v)$ or eyeglass of $G(e)$ are displayed in Figure 5; note that for an eyeglass of $G(e)$ each of these disks meet $\cup\{\tilde{M}_e(i)\colon i = 1,\ldots,2^k+1\}$ in an arc. The comparable disk T for the extra dangle attached to certain of the eyeglasses of $G(e)$ is displayed in Figure 5 and it also

meets $\cup\{\tilde{M}_e(i)\colon i = 1,\ldots,2^k + 1\}$ in an arc. For each edge e of $\mathscr{C}(k-1)$, the core $H(e)$ together with the B's associated with the eyeglasses of $G(e)$ determines disks on $\cup\{\tilde{M}_e(i)\colon i = 1,\ldots,2^k + 1\}$ described in Figure 14. The disks denoted by S's have boundaries composed of a subarc of an eyeglass and a subarc of an arc $B \cap [\cup\{\tilde{M}_e(i)\colon i = 1,\ldots,2^k + 1\}]$ and split into two types, those called *free* S*'s* that are contained in $\cup\{(M_e \cap e)(i)\colon i = 1,\ldots,2^k + 1\}$ and those called *nonfree* S*'s* that arise from an eyeglass that, with its associated B's, links an annular region of a $(M_e \cap e)(i)$ determined by a torus chamber of e. Both free and nonfree S's have boundaries consisting of a subarc of an eyeglass and a subarc of a $B \cap [\cup\{M_e(i)\colon i = 1,\ldots,2^k + 1\}]$ and each has a subarc of a $B \cap [\cup\{M_e(i)\colon i = 1,\ldots,2^k + 1\}]$ hanging into its interior (and no other intersections with B's). The interior of a free S has no intersections with any of the $H(e)$'s or $H(v)$'s while the interior of a nonfree S will have such intersections (we could be more specific about the latter intersections but it is not necessary). The disks denoted by R's have frontiers composed of subarcs from consecutive eyeglasses, the arcs attaching these eyeglasses to J_{k-1}, a subarc of J_{k-1}, and a subarc of an arc $B \cap [\cup\{\tilde{M}_e(i)\colon i = 1,\ldots,2^k + 1\}]$. (Be warned that each R that spans a triangular region connecting successive $M_e(i)$'s has some identifications along the arc of J_{k-1} in its frontier. There is no harm in ignoring these identifications in subsequent arguments provided we do not succumb to the temptation to push intersections over this edge of R.) The extra dangles attached to eyeglasses associated with disk chambers of an $(M_e \cap e)(i)$ that follow an annulus chamber cause there to be three types of R's, these being displayed in Figure 15. Each R has a single intersection of the form $R \cap B$ that is an arc meeting

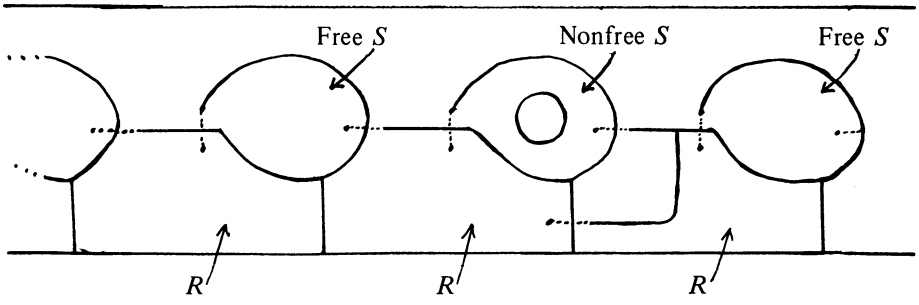

FIGURE 14

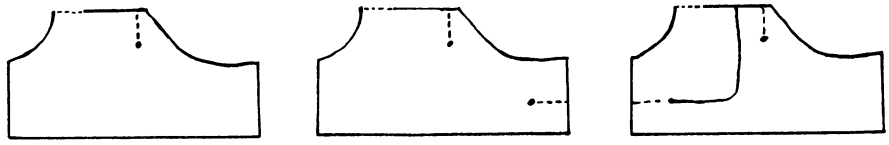

R of type (i) R of type (ii) R of type (iii)

FIGURE 15

the boundary of R is an endpoint. Each R immediately preceding an extra dangle has a single intersection of the form $R \cap T$ that is an arc meeting the boundary of R in an endpoint. Each R immediately "below" an extra dangle contains the stem of the dangle and a single intersection of the form $R \cap T$ that is an arc meeting the boundary of R in an endpoint and meeting the stem of the dangle.

We now verify condition (9) of the preceding section and, even more, the claim in the Main Theorem that each subarc of J is cellular. The totality of the cores of the edges of $\mathscr{C}(k)$, namely,

$[\cup\{H(e)\colon e \text{ an edge of } \mathscr{C}(k-1)\}] \cup [\cup\{H(v)\colon v \text{ a vertex of } \mathscr{C}(k-1)\}]$, can be described as the union of pieces where each piece consists of a subarc of J_{k-1} which is attached at an interior point to an endpoint of an arc that has an eyeglass, possibly with an extra dangle, attached to its other endpoint. These pieces are circularly ordered. The two subarcs of J_{k-1} contained in successive pieces either share a common endpoint (the pieces being contained in the same $H(e)$) or are connected by a subarc of J_{k-1} that determines a vertex of $\mathscr{C}(k)$. Let E denote the union of any consecutive string of such pieces together with the subarcs of J_{k-1} connecting successive pieces that do not meet such that the string *does not contain all the pieces* and let $\overline{E}$ denote the union of E and the B's and T's associated with eyeglasses and dangles contained in E. Note that $\overline{E}$ is connected. Then evident from the description of the $H(e)$'s and $H(v)$'s is that, for any neighborhood U of $\overline{E}$, there is an inclusion

$$E \subset \text{PL 3-cell} \subset U.$$

This property is sufficient to imply that each subarc of J is cellular.

4. Minimal counterexample disks. To each pair of disjoint PL meridional disks D and E of the solid torus K, that are in general position with respect to the $H(e)$'s, $H(v)$'s, B's, T's, R's, S's, $\tilde{M}_e(i)$'s etc. specified during the construction of $\mathscr{C}(k)$, we associate a measure of complexity $C(D, E) = (a_1, a_2, a_3, a_4)$ that is a quadruple (with lexicographical ordering) determined by insisting that:

a_1 is the total number of the components of $[(D \cup E) \cap B]$'s and $[(D \cup E) \cap T]$'s;

a_2 is the total number of components of $[\alpha \cap R]$'s and $[\alpha \cap S]$'s for all components α of a $(D \cup E) \cap B$ or $(D \cup E) \cap T$;

a_3 is the total number of components of $[(D \cup E) \cap S]$'s; and

a_4 is the total number of components of $[(D \cup E) \cap R]$'s.

We shall establish that the collection

$$\{H(e)\colon e \text{ an edge of } \mathscr{C}(k-1)\} \cup \{H(v)\colon v \text{ a vertex of } \mathscr{C}(k-1)\}$$

has the Two Disks Property with respect to K by hypothesizing the existence of counterexample disks D and E and, in the closing paragraph of this section, arrive at the contradiction that they are not counterexample disks. Evidently, small general position adjustments do not compromise counterexample disks so that we assume that D and E are in general position with sets listed in the previous paragraph and, further, that their complexity $C(D, E)$ is the minimum attained by any pair of counterexample disks. We proceed to list and verify fifteen facts related to D and E with the fifteenth being that they are not counterexample disks.

Fact (1). Each component of a $(D \cup E) \cap B$ (resp., $(D \cup E) \cap T$) is a simple closed curve that meets any R or S in at most one point; furthermore, the disk on B (resp., T) that it bounds contains the center point of B (resp., T). (Each Int B and Int T meets exactly one $H(e)$ or $H(v)$, the intersection being a single point called the *center point*.)

If there were simple closed curves of intersection bounding disks on B (resp., T) not containing the center point, then an innermost such simple closed curve and the disk it bounds could be used to perform a disk trade on one of D or E, producing new counterexample disks with smaller complexity. If there were spanning arcs of intersection, an innermost one could be "slid" off B (resp., T) producing a new pair of counterexample disks with smaller complexity. A type T disk meets exactly two R's (and no S's), say R and R'. The intersections $T \cap R$ and $T \cap R'$ are arcs spanning from ∂T to the center point of T meeting only at the center point of T. Each component of $(D \cup E) \cap T$ is a simple closed curve that winds around the center point of T once. If any of these simple curves met either $(T \cap R)$ or $(T \cap R')$ in more than a single point, then an isotopy supported in a "thin" neighborhood of the annular region that is T with small neighborhoods of ∂T and the center point of T removed could be used to produce counterexample disks whose complexity has first coordinate equal to that of $C(D, E)$ but has second coordinate smaller than that of $C(D, E)$. The same argument shows that each component of a $(D \cup E) \cap B$ meets any R or S in at most one point. (While every T meets exactly two R's and most B's meet exactly one R and one S, those B's near an eyeglass $G(v)$ for v a vertex of $\mathscr{C}(k-1)$ meet no R's and at most one S.)

Fact (2). Each component of a $(D \cup E) \cap R$ (resp., $(D \cup E) \cap S$) that meets a B or T is a spanning arc of R (resp., S).

If α is a component of a $(D \cup E) \cap R$ such that $\alpha \cap B \neq \varnothing$, and $B \cap R \not\subset \partial R$ (otherwise, α is clearly a spanning arc), then specify $x \in \alpha \cap B$ and a component α' of $(D \cup E) \cap B$ with $\alpha' \cap \alpha = \{x\}$. Fact (1) assures a single point of intersection and that α' is a simple closed curve. Since B and R meet "transversely", if α were a simple closed curve, then a regular neighborhood of $\alpha \cup \alpha'$ in $D \cup E$ would be a punctured torus contained in a disk; clearly an impossibility. The other cases hold for the same reason.

Fact (3). Each component of a $(D \cup E) \cap (\text{free } S)$ (resp., $(D \cup E) \cap R$) is a spanning arc of S (resp., R).

Fact (2) assures that each component meeting a B or T is a spanning arc. If there were simple closed curve components, then an innermost one would bound a disk missing all $H(v)$'s and meeting $H(e)$'s only along the stem of a dangle (for all R's but only for free S's). This disk could be used to do a disk trade that would produce counterexample disks with smaller complexity.

Fact (4). Each component α of a $(D \cup E) \cap (\text{free } S)$ (resp., $(D \cup E) \cap R$) has the property that if x and y are distinct points of intersection of α with type B disks (resp., type B or T disks) and the segment on α connecting x and y contains no other point of B's or T's, then x and y do not belong to the same type B disk (resp., type B disk or type T disk).

We treat the case that α is a component of $(D \cup E) \cap$ (free S) and leave the other case to the reader. A component α can meet only the two disks, say B and B', that meet this particular free S. If there were points $x, y \in \alpha \cap B$ such that the interior of the segment on α joining x to y missed both B and B', then the path on α from x to y approaches the arc $B \cap S$ either from the same side (this must be the case if $B \cap S \subset \partial S$) or from opposite sides of $B \cap S$. In the former case, the simple closed curve formed by the segment from x to y on α and the segment from x to y on $B \cap S$ would bound a disk on S missing all $H(e)$'s (except for stems of dangles) and $H(v)$'s. A "slide" across an innermost such disk could be used to produce counter-example disks with smaller complexity. As illustrated in Figure 16(a)–(c), two simple closed curve components of $(D \cup E) \cap B$ would be replaced by a single simple

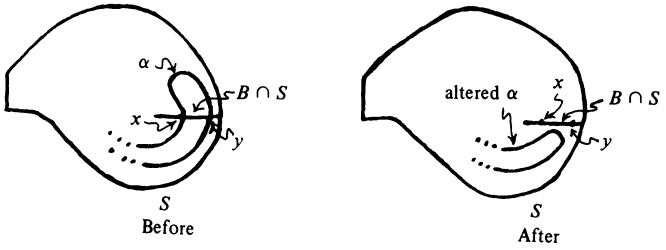

(a) Top View

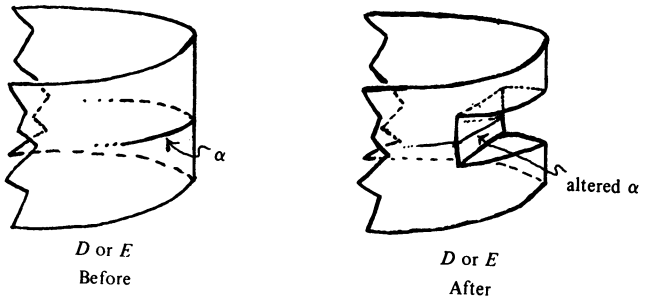

(b) Side view

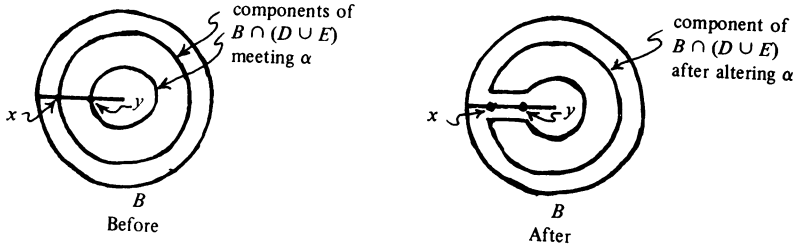

(c) Change in $B \cap (D \cup E)$

FIGURE 16

closed curve component thereby reducing the first coordinate of $C(D, E)$. In the latter case, the same simple closed curve would bound a disk containing the point $\partial B \cap S$, and one of the two closed segments on α complementary to that joining x and y would "run into" the disk. Since it could not wind endlessly around the point $\partial B \cap S$ and would have to exit the disk, it would contain a pair of points of $B \cap \alpha$ that are of the former type.

Fact (5). There is an edge e_0 of $\mathscr{C}(k-1)$ and integers $1 \leqslant t_0 < t_1 < t_2 \leqslant 2^k + 1$ such that both D and E meet each of $\bar{G}(e_0, t_0)$, $\bar{G}(e_0, t_1)$ and $\bar{G}(e_0, t_2)$. Furthermore, should $t_0 = 1$, both D and E meet $\bar{G}(e_0, 1) - \operatorname{Int} B$, where B is the disk associated with the first eyeglass of $G(e_0, 1)$ that meets a $G(v)$. Of course, one of D or E misses $H(e_0)$, say $D \cap H(e_0) = \varnothing$.

The notation introduced in the preceding section included setting $G(e, i)$ equal to the union of the eyeglasses associated with the ith copy, $\tilde{M}_e(i)$, of the disk $\tilde{M}_e$ and setting $\bar{G}(e, i)$ equal to $G(e, i)$ together with the disks B associated with these eyeglasses (e is an edge of $\mathscr{C}(k-1)$ and $i = 1, \ldots, 2^k + 1$). Since $\bar{G}(e, i)$ contains a core of e and the collection of edges of $\mathscr{C}(k-1)$ has the Two Disks Property with respect to K, the collection $\{\bar{G}(e, i)$: e an edge of $\mathscr{C}(k-1)\}$ has the Two Disks Property with respect to K for each $i = 1, \ldots, 2^k + 1$. Since there are only 2^{k-1} edges in $\mathscr{C}(k-1)$, a routine application of the "pigeonhole principle" insures that for some edge, say e_0, there are three integers $1 \leqslant t_0 < t_1 < t_2 \leqslant 2^k + 1$ such that both D and E meet each of $\bar{G}(e_0, t_0)$, $\bar{G}(e_0, t_1)$ and $\bar{G}(e_0, t_2)$. (Since each $\bar{G}(e, 1) - \operatorname{Int} B$ contains a core of e, where B is the disk associated with the first eyeglass of $G(e, 1)$ that meets a $G(v)$, we arrange that both D and E meet $\bar{G}(e_0, 1) - \operatorname{int} B$ in case $t_0 = 1$.)

Fact (6). For each B associated with an eyeglass of $G(e_0)$ (resp., T associated with a dangle of $H(e_0)$) that meets $D \cup E$ but does not meet a $G(v)$ (i.e., not the B associated with the first eyeglass of $G(e_0, 1)$ that meets a $G(v)$), the innermost and outermost components of $(D \cup E) \cap B$ (resp., $(D \cup E) \cap T$) are contained in D.

If such a component were contained in E, then E could be adjusted so as to remove the component thereby producing counterexample disks having smaller complexity.

Fact (7). The disk D meets every B and T that meets a $G(e_0, i)$ for $i < t_2$ except possibly the B associated with the first eyeglass of $G(e_0, 1)$ that meets a $G(v)$.

Since $D \cap \bar{G}(e_0, t_2) \neq \varnothing$ but $D \cap G(e_0, t_2) = \varnothing$ (as $D \cap H(e_0) = \varnothing$), D meets at least one B associated with an eyeglass of $G(e_0, t_2)$. Based on the knowledge of $D \cap B$'s and $D \cap T$'s from Fact (1) and $D \cap R$'s and $D \cap S$'s from Fact (2) and the disjointness of D and $H(e_0)$, the portrayal in Figure 17 is of intersections of D with B's and T's meeting $G(e_0)$ forcing intersections of D with preceding B's and T's. Following this process back to the first eyeglass of $G(e_0, 1)$ starting from the nonempty intersection of D with a B associated with a eyeglass of $G(e_0, t_2)$, establishes Fact (7).

Fact 8. If B (resp., T) is associated with an eyeglass of $G(e_0)$ (resp, dangle of $H(e_0)$) and does not meet a $G(v)$ and $B \cap D \neq \varnothing$ (resp., $T \cap D \neq \varnothing$), then E misses one of the two components of $H(e_0) - B$ (resp., $H(e_0) - T$).

Let α be the innermost simple closed curve of intersection of $(D \cup E) \cap B$, Fact (6) assuring that $\alpha \subset D \cap B$. Form a 2-sphere in K by using the disk on D bounded by α and the disk on B bounded by α. The 3-cell bounded by this 2-sphere misses E and contains one component of $H(e_0) - B$. The same argument works for a type T disk.

Fact (9). The disk E misses one of $G(e_0, t_0)$ or $G(e_0, t_1)$; there will be no loss of generality in assuming $E \cap G(e_0, t_0) = \varnothing$.

Each B whose center point is contained in $G(e_0, t_1)$ (resp., T that meets $G(e_0, t_1)$) splits $H(e_0)$ into two components, a "small" one that is half an eyeglass possibly with a dangle attached (resp., that is an eyeglass with a stem) and a "large" one that contains $G(e_0, t_0)$. Fact (8) assures that E misses one of these two components, were it ever the "large" component, then E would miss $G(e_0, t_0)$ and we would be done. Otherwise, E misses all the small components and, consequently, misses most of $G(e_0, t_1)$. Specifically, E can only meet the subarcs of eyeglasses of $G(e_0, t_1)$ that equal (free S) $\cup$ ($R \cup R'$) as depicted in Figure 18. [The small component associated with a type T disk contains the comparable subarc for a nonfree S, so E must miss such a subarc. The argument that follows showing that E in fact misses the subarcs (free S) $\cap$ ($R \cup R'$) does not work for nonfree S's and, for this reason alone, we were forced to insert the extra dangles. If we had placed dangles on every eyeglass then we could immediately conclude that E misses $G(e_0, t_1)$ but, surprisingly, these additional dangles cause problems later in the argument where we make

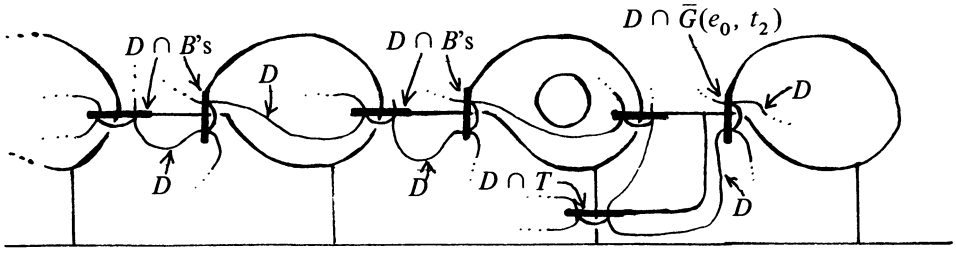

FIGURE 17

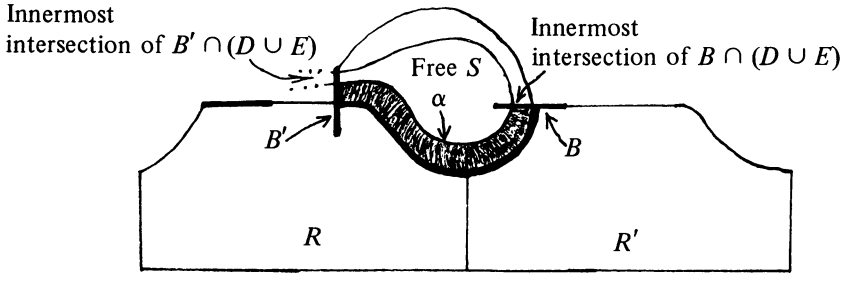

FIGURE 18

use of the fact that most R's intersect no T's. Possibly, no dangles are necessary but we have been unable to verify Fact (9) or a satisfactory replacement without them.] For a free S meeting $G(e_0, t_1)$, as depicted in Figure 18, D meets B (see Fact (7)) and the innermost intersection of $D \cap B$ meets S in a point that determines a component α of $D \cap S$; Facts (3) and (4) ensure that α as well as every other component of $D \cap S$ sit in S as pictured. In particular, $\alpha \cap B'$ determines the innermost intersection of $D \cap B'$. Since the innermost intersections of $(D \cup E) \cap B$ and $(D \cup E) \cap B'$ are contained in D (see Fact (5)), any component of $E \cap S$ meeting $S \cap (R \cup R')$ would be contained in the shaded region of S in Figure 18. Since S is free, the shaded region is free of intersections with $H(e)$'s and $H(v)$'s. Thus "slides" could be performed changing E and producing counterexample disks having smaller complexity.

Fact (10). For a component α of $E \cap R$, where $R \cap G(e_0, t_0) \neq \varnothing$,

(a) if α meets a B, then an endpoint of α lies in a B, and

(b) if an endpoint of α is contained in a B, then there is a nonendpoint of α contained in a B or T.

As displayed in Figure 19, there are three types of R's. A component α of $E \cap R$ satisfies a much stronger property for type (i) and (iii) R's, namely, adopting the notation of Figure 19,

(*) if the component α meet either B' or B'', then both endpoints of α are in B' and α meets B'' in exactly one point.

The stronger property (*) is a consequence of Facts (2), (4) and (6). Suppose α is a component of $E \cap R$ and R is of type (ii). The proof of Fact (9) reveals that there is an arc $\beta \subset \partial R$ (since a type (ii) R occurs only near tori chambers, there are no identifications along $R \cap J_{k-1}$) such that β misses E and contains $(T \cup B'') \cap \partial R$ along with one endpoint of $B' \cap \partial R$ (see Figure 19). Fact (7) assures that D meets each B and T meeting R. Fact (3) states that components of $D \cap R$ are spanning arcs of R, their endpoints lying in $B' \cap \partial R$ as $D \cap H(e_0) = \varnothing$. In particular, as outermost components of $(D \cup E) \cap B$'s and $(D \cup E) \cap T$'s are contained in D for such B's and T's, the points of $H(e_0)$ contained in the interior of R can be joined to $B' \cap \partial R$ missing $E \cap R$. A component α of $E \cap R$ is a spanning arc of R (see Fact (3)) and, consequently, were α to violate (a), then there would be an arc γ in $\partial R - (\beta \cup (B' \cap \partial R))$ such that $\gamma \cup \alpha$ bounds a disk in R. Then $(B'' \cup T) \cap R$

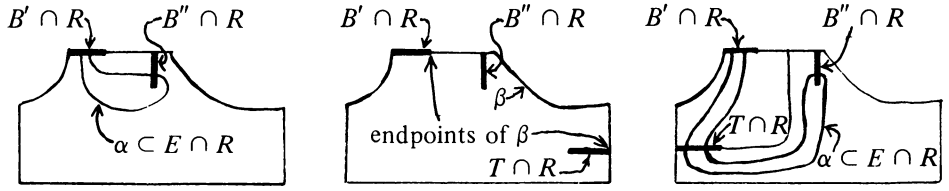

R of type (i) *R* of type (ii) *R* of type (iii)

FIGURE 19

would meet this disk in spanning arcs and an innermost one would reveal a violation of Fact (4). If α were to violate (b), Fact (3) places one endpoint of α in $B' \cap \partial R$ and Fact (4), together with $\beta \cap E = \varnothing$, places the other endpoint in $\partial R - (\beta \cup (B' \cap \partial R))$. Hence, α separates the center point of B' from $(B'' \cup T) \cap R$ in R, an impossibility as innermost intersections of $(D \cup E) \cap B'$ are contained in D and each component of $D \cap R$ meets $(T \cup B'') \cap R$.

Fact (11). If E meets a $\hat{B} \subseteq \overline{G}(e_0, t_0)$ and the center point of $\hat{B}$ is contained in $G(e_0, t_0)$ (i.e., should $t_0 = 1$, $\hat{B}$ is not the disk associated with the first eyeglass that meets a $G(v)$), then E meets all B's contained in $\overline{G}(e_0, t_0)$ that precede $\hat{B}$ until a nonfree S is encountered (should $t_0 = 1$, E might not meet the disk associated with the first eyeglass that meets a $G(v)$) and all B's succeeding $\hat{B}$ until a nonfree S is encountered.

Part (a) of Fact (10) together with Fact (3) (and $E \cap G(e_0, t_0) = \varnothing$) permits us to follow a nonempty intersection $E \cap \hat{B}$ to the "left" until a nonfree S is encountered detecting along the way the nonempty intersections $E \cap B$ claimed. (The argument detects that E meets every disk $B \subset \overline{G}(e_0, t_0)$ whose center point is in $G(e_0, t_0)$ that precedes $\hat{B}$ but we shall not use the additional information.) Similarly using part (b) of Fact (10) the nonempty intersection $E \cap \hat{B}$ can be followed to the "right" until the R is reached that immediately precedes a nonfree S and E meets a type T disk (see Figure 20). Adopting the notation of Figure 20, if E meets B, then part (b) of Fact (10) states that E meets one of B' or T. A simple closed curve of intersection $E \cap T$ determines a component of $E \cap R'$ that meets B''. In turn, a simple closed curve of intersection of $E \cap B''$ determines a component of $E \cap S$ that meets B', thus detecting that E meets B' regardless of whether part (b) of Fact (10) yields an intersection with B' or an intersection with T. (Notice we have not ascertained that there is an intersection of E with B''; consequently, we must stop upon encountering a nonfree S.)

Fact (12). There is a string of $k + 2$ eyeglasses of $G(e_0, t_0)$, say $z_0, z_1, \ldots, z_{k+1}$, and associated disks, say $B_0, \ldots, B_{2(k+1)}$, as in Figure 21 such that each S associated with a z_i, $i = 0, \ldots, k + 1$, is free and such that $E \cap B_i \neq \varnothing$, $i = 0, \ldots, 2(k + 1)$.

Fact (5) states that $E \cap \overline{G}(e_0, t_0) \neq \varnothing$, while Fact (8) states that $E \cap G(e_0, t_0) = \varnothing$. Consequently, there must be a disk $\hat{B}$ as in Fact (11) thereby producing the

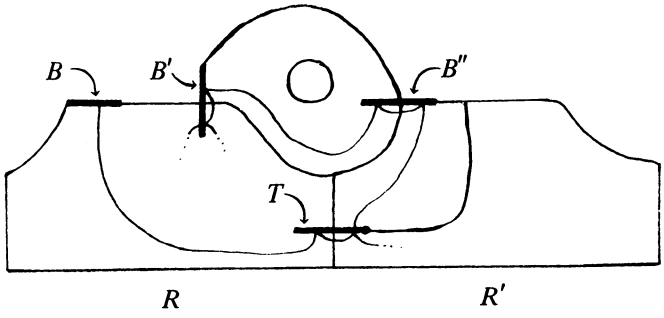

FIGURE 20

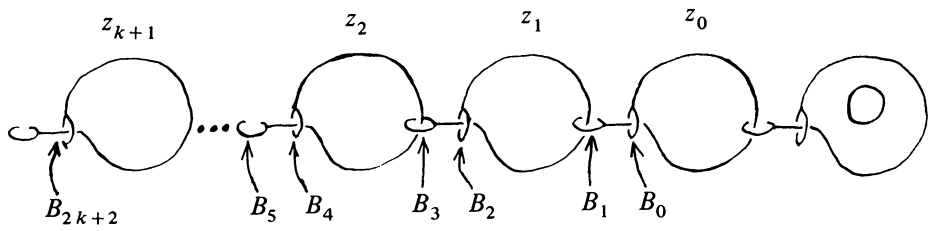

FIGURE 21

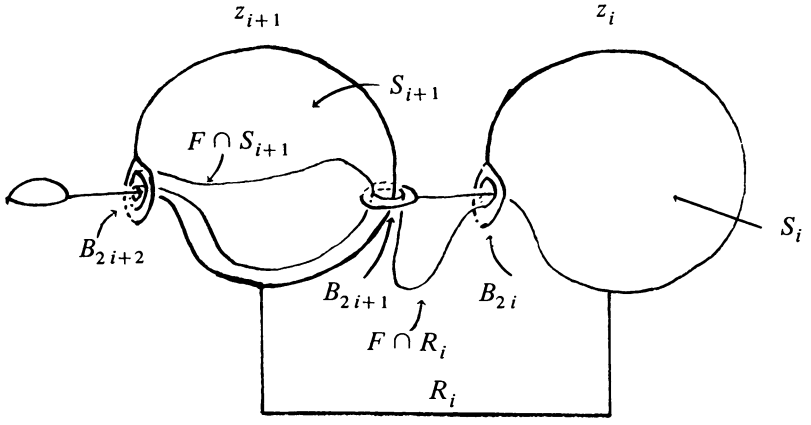

FIGURE 22

sought-after string of eyeglasses. (Recall that Fact (5) assures that, should $t_0 = 1$, $\hat{B}$ is as in Fact (11).) That there is at least $k + 2$ results from our insistence, while describing the edges of $\mathscr{C}(k)$ in the last section, that there be at least $k + 2$ 3-cell chambers of $\mathscr{C}(k-1)$ following and preceding each torus chamber.

Fact (13). For consecutive eyeglasses z_i, z_{i+1}, $0 \leqslant i < k + 1$, a subdisk F of D (resp., E) that is innermost on D (resp., E) with respect to intersections with B_{2i} has precisely the intersections with B_{2i+1} and B_{2i+2} depicted in Figure 22.

Sketched in Figures 23 and 24 is exactly the manner that F meets B_{2i}, B_{2i+1}, B_{2i+2}, R_i, S_i, and S_{i+1}. (The arc $F \cap R_i$ cannot leave from the other side of $R_i \cap B_{2i}$ as a simple linking argument would require $F \cap \mathbf{Z}_i \neq 0$.) Evidently, Fact (13) is true provided these are the precise intersections. Note that the simple closed curve $F \cap B_{2i+1}$ is arcwise accessible on $F - (F \cap B_{2i+2})$ to ∂F and separates on F the pair of simple closed curves $F \cap B_{2i+2}$. The argument verifying Fact (11) shows that any additional intersections of F with either B_{2i+1} or B_{2i+2} could be traced back thereby detecting an additional intersection with $F \cap B_{2i}$, contradicting the choice of F.

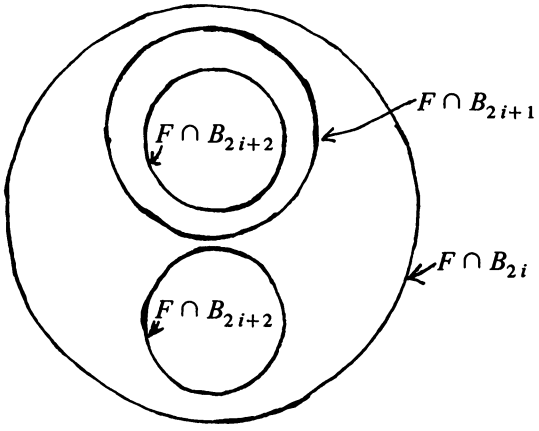

FIGURE 23

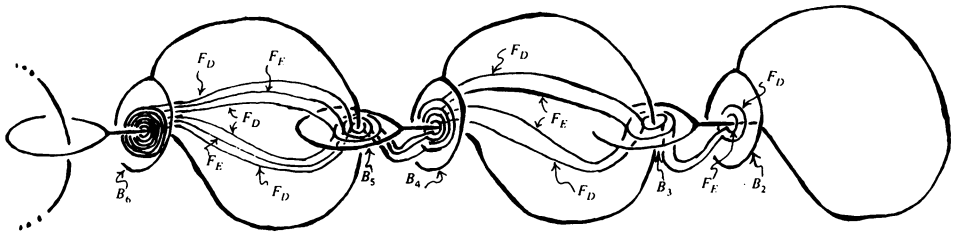

FIGURE 24

Fact (14). There are $t = 2^k + 1$ disks $F_1, \ldots, F_t$ satisfying:

(a) each $F_1, F_3, \ldots, F_{2i+1}, \ldots, F_t$ is innermost on D with respect to intersections with $B_{2(k+1)}$ and $F_2, F_4, \ldots, F_{2i}, \ldots, F_{t-1}$ are innermost on E with respect to intersections with $B_{2(k+1)}$; and

(b) the F_i's are ordered according to the nesting of their boundaries on $B_{2(k+1)}$, ∂F_1 being closest to the center point of $B_{2(k+1)}$.

If F is a subdisk of either D or E that is innermost with respect to intersections with B_2, then repeated applications of Fact (13) detect 2^k subdisks of F innermost with respect to intersections with $B_{2(k+1)}$. If F_E and F_D are subdisks of E and D, respectively, and the boundary of F_E is inside the boundary of F_D on B_2, then from these 2^k subdisks of F_D and 2^k subdisks of F_E there are $2^k + 1$ that satisfy (a) and (b) of Fact (14). Figure 24 illustrates the situation for the first few steps. Notice that while there are four disks at B_4, the largest family that alternates between being from D and from E has only three members. These three produce six disks at B_6 but we can use only five to form a family of disks alternating between disks from D and disks from E. In general there is a family of $2^{i-1} + 1$ disks at B_{2i} that alternates

between disks from D and disks from E with the innermost and outermost from D. Fact (4) is established provided there are disks F_E and F_D as above with the boundary of F_E inside the boundary of F_D on B_2 (there must be disks but their order may be wrong). Backing up to B_0, there are disks $\hat{F}_E$ and $\hat{F}_D$ on E and D, respectively, innermost with respect to intersections with B_0. Regardless of which is inside the other, from amongst the two subdisks of F_E and two subdisks of F_D at B_2 assured by Fact (13) is a desired pair.

Fact (15). Each F_i, $i = 1,\ldots,2^k + 1$, meets a distinct element of $\{H(e)$: e an edge of $\mathscr{C}(k-1)\} \cup \{H(v)$: v a vertex of $\mathscr{C}(k)\}$. Of course, this is absurd since there are only 2^k such elements, the absurdity revealing that E and D cannot be counterexample disks and implying the long sought after Two Disks Property with respect to K of the above collection of elements.

For each $i = 1,\ldots,t = 2^k + 1$, let C_i be the 3-cell bounded by F_i and the subdisk of $B_{2(k+2)}$ bounded by ∂F_i that does not contain $\partial B_{2(k+1)}$. The C_i's are nested with $C_1 \subset C_2 \subset \cdots \subset C_t$. Each F_i meets some $H(e)$ or $H(v)$ since it must meet some eyeglass used in forming the $G(e)$'s and $G(v)$'s. (Recall that $\overline{G}$, the union of all these eyeglasses together with their associated B's, contains a simple closed curve that meets each eyeglass in a subarc and winds once around K. Each ∂F_i links the simple closed curve and an argument simpler than some we have already omitted reveals that F_i meets some eyeglass.) If $H(e)$ meets F_i and $i < t$, then $H(e) \neq H(e_0)$ as $H(e_0) \subset \operatorname{Int} C_1 \cup (S^3 - C_t)$, the latter a set missing all the F_i's except F_t. Further, $H(e) \subset \operatorname{Int} C_{i+1}$ as $H(e) \cap \partial C_{i+1} = \varnothing$ and, therefore, $H(e) \cap F_j = \varnothing$ for $i + 1 \leqslant j \leqslant t$. Similarly, if $H(v)$ meets F_i and $i < t$, then $H(v) \cap F_j = \varnothing$ for $i + 1 \leqslant j \leqslant t$. In particular, no $H(e)$ or $H(v)$ can meet more than one F_i.

5. Applications. The examples claimed in Corollaries 2–4 are built starting not with the decomposition G described in the Main Theorem but rather with the decomposition $\tilde{G}$ described immediately prior to the statement of Corollary 1. Specifically, $N_{\tilde{G}} = N_G - \{g_0\}$, where g_0 is any element of N_G. Choose an arc A' on the disk Q (specified in the Main Theorem) that meets the boundary of Q only in its endpoints, these also being the endpoints of $A = \mathrm{CL}(\bigcup\{g \in N_{\tilde{G}}\})$. Then the subdisk $\tilde{Q}$ of Q bounded by $A \cup A'$ is cellular, for $\tilde{Q}$ is locally tame except at points of A and, thus, there is an ambient isotopy of S^3 fixed on A and outside any prescribed neighborhood of $\tilde{Q}$ that moves $\tilde{Q}$ into any prescribed neighborhood of A. This implies that $\tilde{G}$ satisfies the additional properties claimed in Corollary 3.

Decompositions as described in Corollary 2 are built from $\tilde{G}$ and the disk $\tilde{Q}$ just described as follows. For each $g \in N_{\tilde{G}}$, specify a disk $D_g \subset \tilde{Q}$ such that $D_g \cap \partial\tilde{Q} = g$, $D_g \cap D_{g'} = \varnothing$ for $g \neq g'$, and the D_g's form a null sequence. The decomposition G' whose nondegenerate elements are precisely these D_g's is the first of those described in Corollary 2. Since the D_g's are locally tame except at points of g, the decomposition is equivalent to $\tilde{G}$ in the strongest possible sense. (For example, there is a cell-like map π: $S^3 \to S^3$ such that $\pi(G') = \pi(\tilde{G})$ with $\pi(D_g) = g$ for each $g \in N_{\tilde{G}}$.) In particular, the decomposition spaces S^3/G' and $S^3/\tilde{G}$ are homeomorphic.

The second example described in Corollary 2 is produced by using the local flatness of interior points of each disk D_g to construct a "parallel" disk $\tilde{D}_g$ that meets

D_g only in their common boundaries. The sphere $D_g \cup \tilde{D}_g$ then bounds a 3-cell and, exercising care to keep 3-cells for different $g \in N_{\tilde{G}}$ disjoint and to preserve the nullness, the totality of such 3-cells form the nondegenerate elements of a decomposition. The observation detecting G' to be nonshrinkable also detects that this decomposition is not shrinkable. The global 3-cell containing the 3-cells determined by the D_g's is determined in the same manner using the disk $\tilde{Q}$.

The relevance of the example described in Corollary 4 is to work in [**DE**$_1$, **DE**$_2$, **Da**$_2$, **Da**$_3$], and [**Ba**] which address, among other things, the question of which decompositions as described in Corollary 4 are shrinkable. Specifically, every disk D in S^n satisfies the property that, for a dense G_δ subset of the space of homemorphisms from I^2 onto D, the decomposition as described in Corollary 4 is shrinkable [**DE**$_1$, **DE**$_2$]. For two-dimensional disks in S^n, $n \geqslant 5$, that are cellular, the conclusion is valid for all homeomorphisms [**Da**$_2$]. The example cited in Corollary 4 and described below reveals that the latter result does not extend to dimension three. The starting point again is the decomposition $\tilde{G}$ and the disk $\tilde{Q}$. Use the local tameness, as before, of $\tilde{Q}$ except at points of the subarc of its boundary $A = \mathrm{CL}(\bigcup\{g \in N_{\tilde{G}}\})$ to produce a "parallel" disk $\hat{Q}$ that meets $\tilde{Q}$ precisely along A, contains A in its boundary, and is locally tame except at points of A. The two-cell $\tilde{Q} \cup \hat{Q}$ is cellular and admits a homeomorphism, say e: $I^2 \to \tilde{Q} \cup \hat{Q}$, for which the decomposition H determined by $N_H = \{e(I \times \{t\})\colon 0 \leqslant t \leqslant 1\}$ is not shrinkable. Specifically, e can be any homeomorphism for which each element $g \in N_{\tilde{G}}$ is contained in a distinct level set $e(I \times \{t\})$. The reason such an H is not shrinkable is that $\tilde{Q} \cup \hat{Q}$ is locally tame except at points of A. The important detail is that if $D \subset I^2$ is a subdisk meeting each $I \times \{t\}$ in an arc with $\mathrm{CL}(\bigcup\{g \in N_{\tilde{G}}\}) \subset e(D)$, then the decomposition H' determined by $N_{H'} = \{e(D \cap I \times \{t\})\colon 0 \leqslant t \leqslant 1\}$ is equivalent to the decomposition H (in the sense specified earlier). The shrinkability of H and, consequently, of all such H' would provide the necessary "shrinking" homeomorphisms to shrink the nonshrinkable decomposition $\tilde{G}$.

References

[**Ar**] S. Armentrout, *Cellular decompositions of 3-manifolds that yield 3-manifolds*, Mem. Amer. Math. Soc. No. 107 (1971).

[**Ba**] C. D. Bass, *Squeezing m-cells to (m − 1)-cells in E^n*, Fund. Math. **110** (1980), 35–50.

[**Bi**] R. H. Bing, *Point-like decompositions of E^3*, Fund. Math. **50** (1962), 431–453.

[**BS**] R. H. Bing and M. Starbird, *A decomposition of S^3 with a null sequence of cellular arcs*, Geometric Topology (J. C. Cantrell, ed.), Academic Press, New York, 1979, pp 3–21.

[**Da**$_1$] R. J. Daverman, *A nonshrinkable decomposition of S^n determined by a null sequence of cellular sets*, Proc. Amer. Math. Soc. **75** (1979), 171–176.

[**Da**$_2$] _____, *Shrinking certain closed 1-dimensional decompositions of manifolds*, Houston J. Math. **5** (1979), 41–47.

[**Da**$_3$] _____, *On cells in Euclidean space that cannot be squeezed*, Rocky Mountain J. Math. **5** (1975), 87–93.

[**DE**$_1$] R. J. Daverman and W. T. Eaton, *An equivalence for the embeddings of cells in a 3-manifold*, Trans. Amer. Math. Soc. **145** (1969), 369–381.

[**DE**$_2$] _____, *A dense set of sewings of two crumpled cubes yield S^3*, Fund. Math. **65** (1969), 51–60.

[**DW**] R. J. Daverman and J. J. Walsh, *A nonshrinkable decomposition of S^n involving a null sequence of cellular sets*, Trans. Amer. Math. Soc. **272** (1982), 771–784.

[**Ed**] R. D. Edwards, *Approximating certain cell-like maps by homeomorphisms*, Notices Amer. Math. Soc. **24** (1977), A-649.

[**Fr**] M. Freedman, *The topology of four-dimensional manifolds*, J. Differential Geom. **17** (1982), 357–453.

[**GM**] D. S. Gillman and J. M. Martin, *Countable decompositions of E^3 into points and point-like arcs*, Notices Amer. Math. Soc. **10** (1963), 74–75.

[**Mc**] D. R. McMillan, Jr., *A criterion for cellularity in a manifold*, Ann. of Math. (2) **79** (1964), 327–337.

[**Wr**] D. G. Wright, *A decomposition of E^n ($n \geqslant 3$) into points and a null sequence of cellular sets*, General Topology Appl. **10** (1979), 297–304.

Department of Mathematics, University of Tennessee, Knoxville, Tennessee 37996 - 1300